Dissolution and Biological Assessment of Cancer-Targeting Nano-ZIF-8 in Zebrafish Embryos

Nurul Akmarina Mohd Abdul Kamal, Emilia Abdulmalek, Sharida Fakurazi, Kyle E. Cordova,
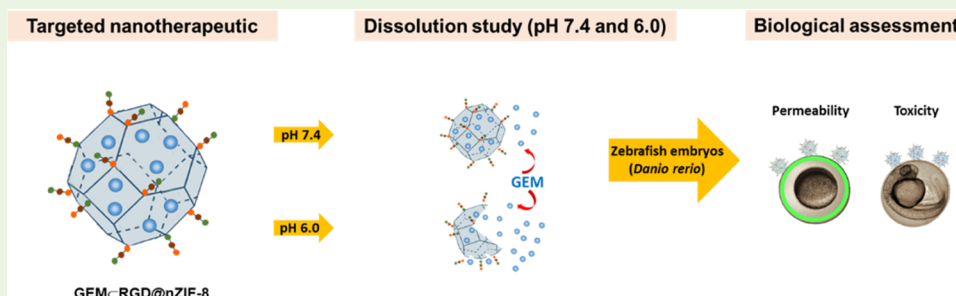and Mohd Basyaruddin Abdul Rahman*

Cite This: https://doi.org/10.1021/acsbiomaterials.2c00186

Read Online

| ACCESS | Metrics & More | Article Recommendations | Supporting Information |

Targeted nanotherapeutic — Dissolution study (pH 7.4 and 6.0) — Biological assessment

ABSTRACT: Cancer-targeting nanotherapeutics offer promising opportunities for selective delivery of cytotoxic chemotherapeutics to cancer cells. However, the understanding of dissolution behavior and safety profiles of such nanotherapeutics is scarce. In this study, we report the dissolution profile of a cancer-targeting nanotherapeutic, gemcitabine (GEM) encapsulated within RGD-functionalized zeolitic imidazolate framework-8 (GEM⊂RGD@nZIF-8), in dissolution media having pH = 6.0 and 7.4. GEM⊂RGD@nZIF-8 was not only responsive in acidic media (pH = 6.0) but also able to sustain the dissolution rate (57.6%) after 48 h compared to non-targeting nanotherapeutic GEM⊂nZIF-8 (76%). This was reflected by the f_2 value of 36.1, which indicated a difference in the dissolution behaviors of GEM⊂RGD@nZIF-8 and GEM⊂nZIF-8 in acidic media compared to those in neutral media (pH = 7.4). A dissolution kinetic study showed that the GEM release mechanism from GEM⊂RGD@nZIF-8 followed the Higuchi model. In comparison to a non-targeting nanotherapeutic, the cancer-targeting nanotherapeutic exhibited an enhanced permeability rate in healthy zebrafish embryos but did not induce lethality to 50% of the embryos ($LC_{50} > 250$ μg mL^{-1}) with significantly improved survivability (75%) after 96 h of incubation. Monitoring malformation showed minimal adverse effects with only 8.3% of edema at 62.5 μg mL^{-1}. This study indicates that cancer-targeting GEM⊂RGD@nZIF, with its pH-responsive behavior for sustaining chemotherapeutic dissolution in a physiologically relevant environment and its non-toxicity toward the healthy embryos within the tested concentrations, has considerable potential for use in cancer treatment.

KEYWORDS: cancer, chemotherapy, targeting nanotherapeutics, reticular chemistry, drug delivery, zebrafish embryo, permeability, toxicity

■ INTRODUCTION

Cancer is one of the leading causes of mortality with a significant number of reported global cases each year.[1] Although chemotherapy plays a vital role in cancer treatment, many non-selective chemotherapeutics are fundamentally limited by dose-dependent toxicity that leads to hair loss, diarrhea, constipation, nausea, vomiting, fatigue, skin problems, hearing loss, and low blood cell counts.[2] For this simple reason, there is an immediate need, and moral obligation, to develop more efficient, selective chemotherapeutic systems that have minimal adverse side effects. A viable strategy for minimizing adverse side effects while maintaining high efficiency and efficacy is to encapsulate the non-selective chemotherapeutics inside a biocompatible nanocarrier whose external surface is functionalized with an arsenal of ligands that are capable of selectively targeting and, thereafter, releasing the chemotherapeutics directly to cancer cells without harming normal cells.

Nanosized zeolitic imidazolate framework-8 (nZIF-8) is widely used as a nanocarrier for chemotherapeutics due to its unique properties such as high loading capacity, surface customizability, and pH-responsive nature for the desired treatment purpose.[3−8] The flexibility of nZIF-8 offers vast opportunities for chemical or ligand surface functionalization to improve chemotherapeutic nanodelivery methods, especially

Scheme 1. Schematic Representation of the Dissolution Study of Gemcitabine (GEM) in Physiologically Relevant Conditions and the Biological Assessment of Permeability and Toxicity of the Cancer-Targeting Nanotherapeutic, RGD-Functionalized GEM-Encapsulated nZIF-8 (GEM⊂RGD@nZIF-8) at Different Incubation Times[a]
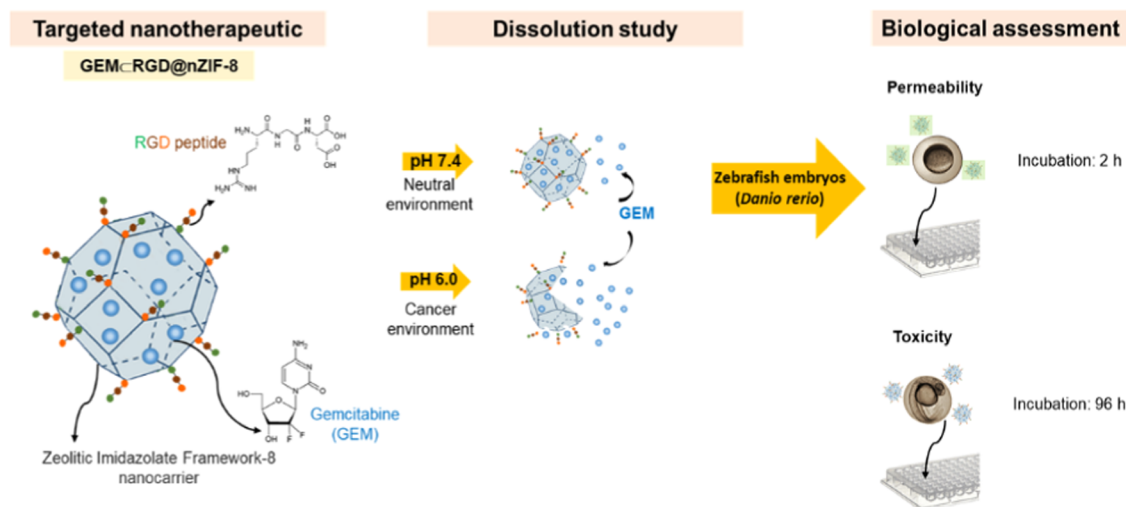
[a]Healthy embryos were transferred to a 96-well round-bottom plate for the biological assessments.

as it pertains to dissolution, selective toxicity, biodistribution, and efficacy.[9−12] As an example, amino-polyethylene glycol-functionalized ZIF-8 demonstrated low toxicity to normal cells when compared to cancer cells as a result of drug retention inside the framework under neutral conditions (pH = 7.4).[13,14] Other ZIF-8 nanodelivery systems based on targeting ligands, such as folic acid and hyaluronic acid, have successfully promoted the uptake and inhibited the growth of cancer cells.[12,15] Our group recently reported an exceptional active-targeting chemotherapeutic system in which gemcitabine (GEM) was encapsulated within RGD-functionalized nZIF-8 (GEM⊂RGD@nZIF-8). This nanotherapeutic system demonstrated selective and active targeting action in delivering the gemcitabine (selective index, SI > 2) toward A549 lung cancer cells with enhanced cellular uptake and apoptotic populations. GEM⊂RGD@nZIF-8 was able to regulate the GEM selectively toward lung cancer cells (A549) while ensuring less harm to healthy lung cells (MRC-5). As the interaction between biological organisms and nanotherapeutics is mediated via their respective surfaces, in our previous study, the surface of nZIF-8 loaded with fluorescein (for uptake) or gemcitabine (for therapy) was surface-functionalized with the RGD homing peptide.[16] RGD on the surface of nZIF-8 was recognized as an important parameter determining the interaction of GEM⊂RGD@nZIF-8 with the biological membranes, thus influencing cellular uptake, toxicity, and apoptotic in cancer cells. It was also known that the safety of nanotherapeutics was related to physicochemical characteristics, including size and surface chemistry.[17] Hence, to gain further insight into the safety and biocompatibility, we determined that there was a need for careful biological assessment to confirm that the interaction of GEM⊂RGD@nZIF-8 with biological membranes caused minimal toxicity effects to otherwise healthy biological functions.

Zebrafish (*Danio rerio*) is a well-established vertebrae animal model for human disease study, including cancer.[18] Many important findings in zebrafish development apply to human development due to high genomic similarities (70%).[19,20] Owing to their smaller size, zebrafish have high reproducibility and rapid embryo development with optical transparency.[21] The transparent protective membrane encircles the embryo, known as a chorion, thereby allowing nanotherapeutics to permeate and be readily visualized.[22,23] Depending on the disease model, various biological aspects including toxicity,[24] hatching,[25] organ development, and behavior[26] can be assessed, all of which support the safety and efficacy assessment of newly developed drug delivery systems.[27−29]

Considering this, our interest herein was to ascertain the ability of a cancer-targeting nanotherapeutic system, gemcitabine encapsulated within RGD-functionalized nZIF-8 (GEM⊂RGD@nZIF-8), to promote permeability through the biological barrier and to assess possible toxicity within healthy zebrafish embryos. Prior to embryo assessment, we also studied the dissolution profile of GEM⊂RGD@nZIF-8 in physiologically relevant environments (Scheme 1). It was worth studying the dissolution profile, as GEM was used in treating not only lung cancer but also other types of cancers, including breast, bladder, and pancreatic.[30] Following the evaluation of the dissolution profile and the biological assessment of this nanotherapeutic's use in healthy embryonic zebrafish, our study provided a deeper insight into the safety of a new nanotherapeutic holding tremendous potential for cancer treatment.

■ MATERIALS AND METHODS

Materials and Supplies. Zinc nitrate hexahydrate (Zn(NO$_3$)$_2$·6H$_2$O; 99% purity), 2-methylimidazole (99% purity), gemcitabine (99% purity), fluorescein (95% purity), *p*-formaldehyde (95% purity), acetonitrile (≥99.9% purity), and triethylamine (99.5% purity) were acquired from Fisher Scientific. Arg-Gly-Asp (RGD) homing peptide was purchased from GL Biochem. Phosphate-buffered saline (PBS) was purchased from Gibco. Acetonitrile (≥99.9% purity) was acquired from Fisher Scientific. Zebrafish embryos (*D. rerio*) and Danio-SprintM embryo media were purchased from Danio Assay Laboratories Sdn. Bhd. (Selangor, Malaysia) that operates under and according to the Institutional Animal Care and Use Committee of Universiti Putra Malaysia.

Equipment. High-performance liquid chromatography (HPLC; Waters Corporation, Milford, Massachusetts) for dissolution study was performed with a C$_{18}$ column (Phenomenex C$_{18}$ column: 3.5 μm,
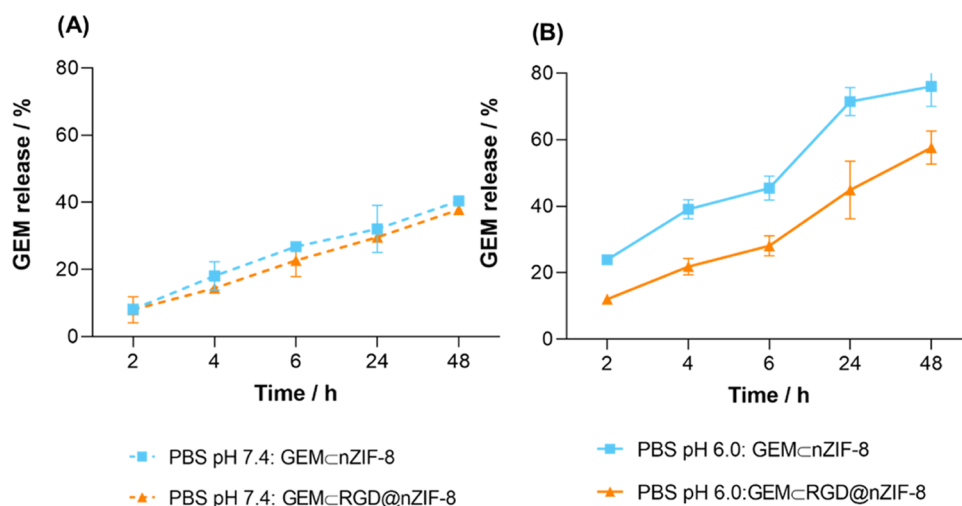
Figure 1. Comparison of GEM dissolution profiles from cancer-targeting GEM⊂RGD@nZIF-8 (orange) and non-targeting GEM⊂nZIF-8 (blue) in (A) PBS media at pH = 7.4 (dashed line) and (B) pH = 6.0 (solid line) at 37 °C over a period of 48 h. Error bars depict standard deviation (n = 2).

4.6×150 mm^2). Fluorescence imaging for permeability was carried out with a Carl Zeiss fluorescence microscope. The images were taken with a Zeiss AxioCam MRm camera and processed with Zen Lite 2012 software. The development of embryos for survival analysis, malformation, and hatching was observed using an inverted microscope (Nikon Eclipse TS100).

Nanotherapeutic Preparation and Characterization. Our previous report details the preparation and characterization of the cancer-targeting nanotherapeutic (GEM⊂RGD@nZIF-8), non-targeting nanotherapeutic (GEM⊂nZIF-8), and pure nano-zeolitic imidazolate framework-8 (nZIF-8) nanosystems used in this work (see Supporting Information (SI), Figures S1–S3).[16]

Gemcitabine (GEM) Dissolution Profile of Cancer-Targeting Nanotherapeutic (GEM⊂RGD@nZIF-8). The dissolution study of GEM was performed in PBS dissolution media (200 μg mL^{-1} in pH = 7.4 and 6.0, respectively) at 37 °C under gentle stirring (100 rpm). At a given time (2, 4, 6, 24, and 48 h), the nanotherapeutics were collected by centrifugation at 11,300g for 10 min to separate the precipitate from the supernatant.[31,32] The supernatant was analyzed by high-performance liquid chromatography (HPLC) at 268 nm with an acetonitrile and water mixture (10:90 v/v) as the mobile phase at a flow rate of 1 mL min^{-1}. The GEM dissolution percentage of all nanotherapeutics was determined as the ratio of the released amount to the total loaded amount of GEM.[31,32]

To compare the dissolution profiles between cancer-targeting GEM⊂RGD@nZIF-8 and non-targeting GEM⊂nZIF-8, a similarity factor (f_2) was measured. The f_2 similarity metric is a function of the reciprocal of the mean square root transform of the sum of square distances. The f_2 similarity metric was calculated as follows (eq 1)[33]

$$f_2 = 50 \log\left\{\left[1 + \frac{1}{n}\sum_{t=1}^{n}(R_t - T_t)^2\right]^{-0.5} 100\right\} \quad (1)$$

where n is the number of time points and R_t and T_t represent the percentage of the GEM released within the comparator curve for non-targeting nanotherapeutic (GEM⊂nZIF-8) and the cancer-targeting nanotherapeutic (GEM⊂RGD@nZIF-8), respectively. The comparison dissolution profiles are similar when the f_2 value is 50–100.[33]

Mathematical models including zero-order (eq 2), first-order (eq 3), Higuchi (eq 4), Hixson−Crowell (eq 5), and Korsmeyer−Peppas (eq 6) were fitted to determine the dissolution kinetics of GEM from GEM⊂nZIF-8 and GEM⊂RGD@nZIF-8 in both dissolution media having pH = 7.4 and 6.0. The model equations are as follows[34−36]

$$M_t = M_0 + k_0 t \quad (2)$$

$$\log M_t = \log M_0 + k_1 t \quad (3)$$

$$M_t = k_H \sqrt{t} \quad (4)$$

$$M_0^{1/3} - M_t^{1/3} = K_w t \quad (5)$$

$$M_t^{1/3}/M_\infty^{1/3} = K_m t^n \quad (6)$$

where M_0 is the initial amount of GEM in the dissolution media; M_t is the amount of GEM in the dissolution media at time t; k_0, k_1, k_H, k_w, and k_m are dissolution rate constants; and M_t/M_∞ is the fraction of GEM released at time t. n is used to characterize different release mechanisms. Finally, the coefficient of determination (R^2) was considered to measure the best-fit model equation, thereby representing the dissolution pattern.

Biological Assessment of Cancer-Targeting GEM⊂RGD@ nZIF-8 on Embryonic Zebrafish (*D. rerio*). The embryos were observed under an inverted light microscope (Nikon Eclipse TS100) to ensure that only viable and healthy embryos were selected for assessments including permeability, toxicity, malformation, and hatching rate. All nanotherapeutics were exposed to 96-well round-bottom plates containing zebrafish embryos via an incubation approach (SI, Figure S4).

Permeability Assessment. For permeability assessment, healthy embryos (aged; 1 h post-fertilization) were loaded at a count of 1 embryo per well in a 96-well round-bottom plate at constant temperature (28 °C). The embryos were incubated with fluorescent fluorescein (Fl) suspensions (Fl as control, Fl⊂RGD@nZIF-8 as the targeting model, and Fl⊂nZIF-8 as the non-targeting model) at a concentration of 50 μg mL^{-1} for 2 h. Following incubation, the embryos were then washed with embryo media. This was followed by visualization via fluorescence microscopy (Carl Zeiss AxioCam MRM). For detection purposes, 517 nm bandpass filters were employed for green fluorescence.

Toxicity, Malformation, and Hatching Assessment. The zebrafish embryotoxicity assessment was carried out following Test No. 236: Fish Embryo Acute Toxicity Test (FET).[37] FET allows for the evaluation of the phenotypes displayed by embryos after chemical treatment. For this study, healthy embryos (aged; 24 h post-fertilization) were transferred to a 96-well round-bottom plate with 1 embryo per well at 28 °C. The embryos were then incubated with the cancer-targeting GEM⊂RGD@nZIF-8, non-targeting GEM⊂nZIF-8, and pure nZIF-8 for 96 h. Concentrations ranging from 0 to 250 μg mL^{-1} were applied with a total of 24 embryos per concentration. A 0.1% dimethyl sulfoxide (DMSO) concentration in each well was maintained, including controls.

C

Survival studies, malformation, and hatching rates of embryos were observed using an inverted microscope (Nikon Eclipse TS100). The observation and scoring were measured as compared with the control. Death, coagulation of embryos, lack of somite formation, non-detachment of the tail, and lack of heartbeat were important parameters to determine embryos or larvae lethality. The lethal concentration (LC_{50}) was calculated using GraphPad Prism 8.0 software. Finally, the hatching rate was calculated as follows (eq 7)[38]

$$\text{hatching rate } (\%) = [\text{number of hatched embryos} \\ /\text{initial number of embryos}] \times 100 \qquad (7)$$

Statistical Data Analysis. All statistical analyses in the experiments described above were analyzed using GraphPad Prism 8.0. Error bars represent the mean values with standard deviation (SD) unless otherwise indicated. The statistical significance level was set at 0.05.

■ RESULTS AND DISCUSSION

Dissolution Profile. The dissolution rate of GEM from cancer-targeting GEM⊂RGD@nZIF-8 and non-targeting GEM⊂nZIF-8 nanotherapeutics was first studied in PBS dissolution media having pH = 6.0 or 7.4. The equation for the GEM standard curve in PBS was $y = 42.902x$, $R^2 = 0.993$ (SI, Figure S5). As shown in Figure 1, both cancer-targeting GEM⊂RGD@nZIF-8 and non-targeting GEM⊂nZIF-8 exhibited a low dissolution percentage of GEM at pH = 7.4 during the first 2 h (8.0 and 8.2%, respectively) but increased drastically after 48 h (37.8 and 40.4%, respectively). In contrast, at pH = 6.0, GEM⊂RGD@nZIF-8 and GEM⊂nZIF-8 displayed fast dissolution of GEM in the first 2 h (12 and 23.9%, respectively), which then increased to 57.6 and 76.0%, respectively, after 48 h. From these findings, we noted that both nanotherapeutics had a higher dissolution rate and responsiveness in an acidic pH environment mimicking that of a tumor microenvironment as compared to a neutral pH environment. Indeed, slow dissociation of the nZIF-8 framework occurred in acidic media due to hydrolysis of the coordination bonds between the Zn(II) metal ions and the 2-methylimidazolate linker. This dissociation promoted drug release slowly at first; however, as more framework was dissociated, the drug was released at an increasingly higher rate.[39−42] This is supported by a previous report that showed that a fast and higher drug dissolution rate from BNZ@ZIF-8 was achieved in acidic media when compared with a media having neutral pH.[43]

The dissolution profiles of cancer-targeting GEM⊂RGD@nZIF-8 and non-targeting GEM⊂nZIF-8 are then compared in dissolution media with either pH = 6.0 or 7.4 by calculating the similarity value (f_2) (Table 1). For this, it is important to note that an f_2 value of 50−100 is considered to be similar and with the dissolution profiles being comparable.[33] In pH = 7.4, an f_2 value of 75.3 was calculated, indicating a similar dissolution rate by cancer-targeting GEM⊂RGD@nZIF-8 and non-targeting GEM⊂nZIF-8 in a neutral pH environment. In pH = 6.0, a calculated f_2 value of 36.1 means that the dissolution

Table 1. Similarity Factor (f_2) of Non-targeting GEM⊂nZIF-8 and Cancer-Targeting GEM⊂RGD@nZIF-8

medium	comparison	f_2[a] value
pH 7.4	GEM⊂nZIF-8 vs GEM⊂RGD@nZIF-8	75.3
pH 6.0	GEM⊂nZIF-8 vs GEM⊂RGD@nZIF-8	36.1

[a]A f_2 value of 50−100 indicates similarity.

profiles are not similar, which correlates with a lower dissolution rate for cancer-targeting GEM⊂RGD@nZIF-8 than non-targeting GEM⊂nZIF-8. Furthermore, it is concluded from this that cancer-targeting GEM⊂RGD@nZIF-8 is better at sustaining GEM dissolution in an acidic environment (pH = 6.0). We surmise that this sustained behavior is due to the RGD-binding effect at the surface of GEM⊂nZIF-8, which improves framework stability in an acidic tumor-like environment.

The dissolution kinetics of GEM were studied via zero-order, first-order Higuchi, Korsmeyer−Peppas, and Hixson−Crowell models with the goal being to elucidate the mechanism of drug transport out of the studied porous nanotherapeutics.[44] From the coefficient of determination (R^2), we found that the Higuchi model was most satisfactory in describing the kinetics of the GEM dissolution process from both cancer-targeting GEM⊂RGD@nZIF-8 and non-targeting GEM⊂nZIF-8 at pH = 6.0 or 7.4 (Table 2 and SI, Figures S6 and S7). The Higuchi model ascribes the rate of water-soluble and low-soluble drugs incorporated within semisolid and solid materials based on the diffusion process according to Fick's law.[35] From these kinetic studies, GEM is proposed to be released from the nZIF-8's framework by the drug leaching through the pore openings upon dissociation of the nZIF-8 framework in acidic media. Indeed, these findings are in agreement with those reported in the literature.[45,46]

Cancer-targeting GEM⊂RGD@nZIF-8 is responsible for elevating cancer outcomes at the cellular level including uptake, cytotoxicity, and apoptosis.[16] Following these outcomes, cancer-targeting GEM⊂RGD@nZIF-8 was studied further to gain deeper insight into the biological effects of its use in healthy small organisms.

Permeability and Toxicity Assessment on Zebrafish Embryos (*D. rerio*). Targeted nanotherapeutics with the potential to reach the exterior cell membrane and promote uptake[16,47,48] require organism-based study to assess safety and viability. The transparency of the zebrafish embryo (*D. rerio*) allows for rapid and clear imaging of fluorescent dyes passing through biological barriers to measuring a nanotherapeutic system's given permeability.[49] To determine the permeability of the cancer-targeting GEM⊂RGD@nZIF-8, we replaced the loaded GEM in RGD@nZIF-8 with a fluorescent dye, fluorescein (Fl), to visualize the dye signal of Fl⊂RGD@nZIF-8 (the fluorescent-tagged cancer-targeting model) and Fl⊂nZIF-8 (fluorescent-tagged non-targeting model) in zebrafish embryos. Embryos (aged; 1 h post-fertilization; hpf) were incubated independently with both Fl⊂RGD@nZIF-8 and Fl⊂nZIF-8 for 2 h, at which time the permeability capacity through the embryos was observed via a fluorescence microscope. It is noted that the permeability of the chorion changes during development.[50,51] Very early age embryos (<1 hpf) are chosen for this study because they are more responsive to chemicals than later ages (4 hpf).[52] The zebrafish embryo without the nZIF-8 incubation (fluorescein, Fl) is shown in Figure 2A. In Figure 2B,C, the fluorescence (Fl) intensity was considerably higher in the zebrafish embryos after 2 h of incubation with Fl⊂RGD@nZIF-8 when compared with Fl⊂nZIF-8. This is strong evidence of the ability of the RGD homing peptide attached to the surface of nZIF-8 to achieve a higher permeability potential through the chorion membrane than the unfunctionalized nZIF-8. Indeed, it is known that specific RGD−integrin interactions take place on the chorion membrane due to the temporal expression of $\alpha v \beta 3$

Table 2. Kinetic Parameters of GEM Dissolution

| | | kinetic model | | | | |
| | | coefficient of determination (R^2) | | | | |
PBS dissolution medium (pH)	nanotherapeutic	zero-order	first-order	Higuchi	Hixson−Crowell	Korsmeyer−Peppas
7.4	GEM⊂RGD@nZIF-8	0.7778	0.8305	0.9340	0.8132	0.7822
	GEM⊂nZIF-8	0.1746	0.7757	0.8903	0.7555	0.7135
6.0	GEM⊂RGD@nZIF-8	0.8415	0.9209	0.9759	0.8971	0.7261
	GEM⊂nZIF-8	0.7005	0.8410	0.9067	0.7996	0.6165
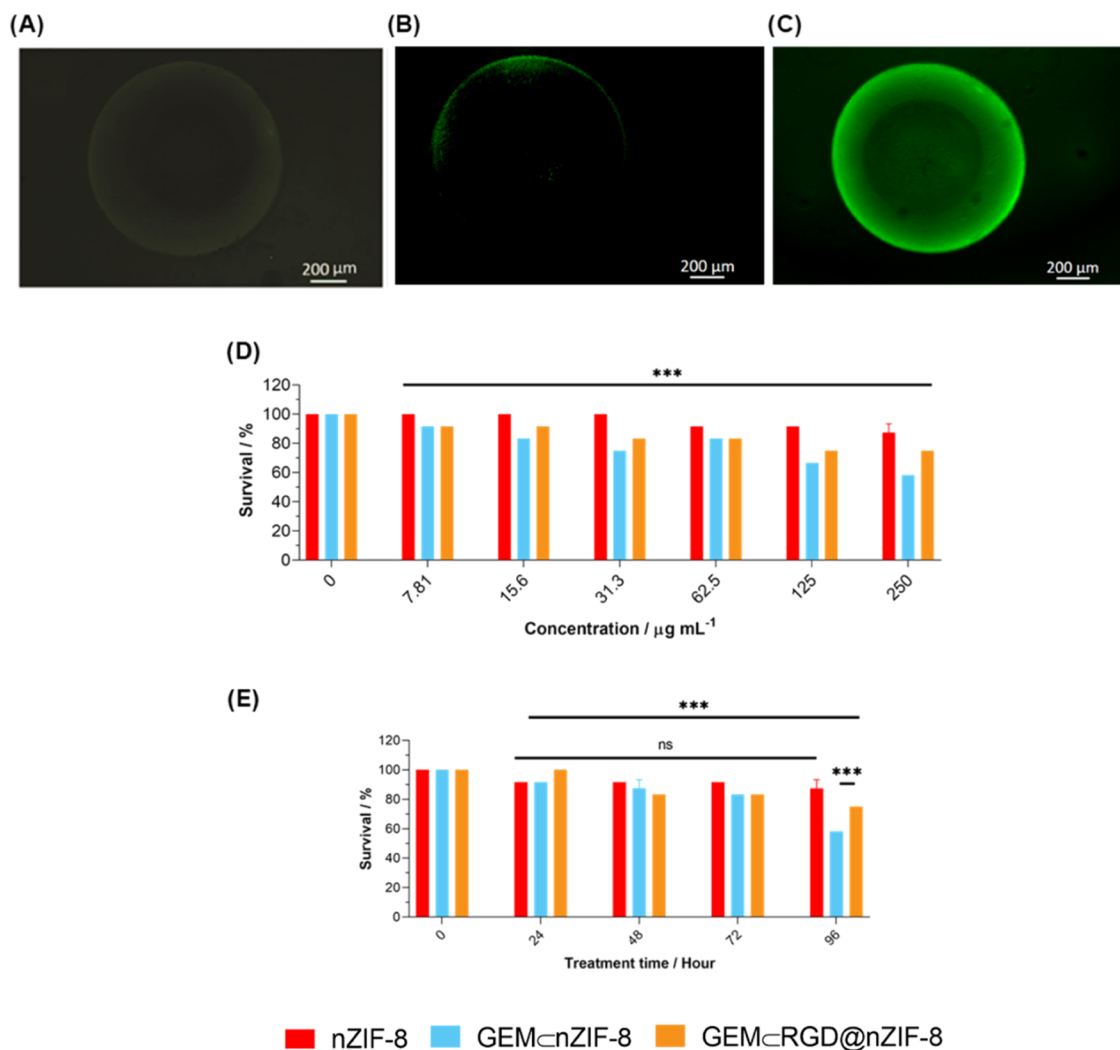
Figure 2. Fluorescence microscopy images for (A) fluorescein (Fl), (B) non-targeting Fl⊂nZIF-8, and (C) cancer-targeting Fl⊂RGD@nZIF-8 comparing the permeability within zebrafish embryos (*D. rerio*). Toxicity was assessed after incubating zebrafish embryos (*D. rerio*) with a total of 24 embryos/concentration with pure nZIF-8 (red), non-targeting GEM⊂nZIF-8 (blue), and cancer-targeting GEM⊂RGD@nZIF-8 (orange) at (D) various concentrations for 96 h and (E) the highest concentration (250 μg mL^{-1}) at 24−96 h of incubation time. Error bars represent standard deviation (*n* = 2). Code: ns = non-significant; and ***$P < 0.001$.

integrins during the early embryonic zebrafish stage.[53−55] Furthermore, the temporal integrins transmit the bidirectional signals across the chorion membranes to activate the ligand-binding through integrin-mediated signaling mechanisms.[56,57] Once activated, the integrins' ectodomains extend to an open state, which leads to high ligand affinity and excellent signal transmission. This subsequently promotes the permeability by an endocytic pathway.[58]

Given that the cancer-targeting GEM⊂RGD@nZIF-8 showed a high permeability across the chorion membrane, we then turned our attention to evaluating potential toxicity

that could result in healthy zebrafish embryos (aged; 24 hpf). Studies have reported that early age fish and invertebrates are far more sensitive to toxins than adult organisms.[59,60] This is because the toxins may take less time to reach the organ at an early age due to their smaller size than at later ages and adults. Accordingly, the embryos were incubated with various concentrations of cancer-targeting GEM⊂RGD@nZIF-8, non-targeting GEM⊂nZIF-8, and pure nZIF-8 as a control. As displayed in Figure 2D, toxicity was assessed by calculating the survival percentage at 96 h post-incubation. From these experiments, cancer-targeting GEM⊂RGD@nZIF-8, non-
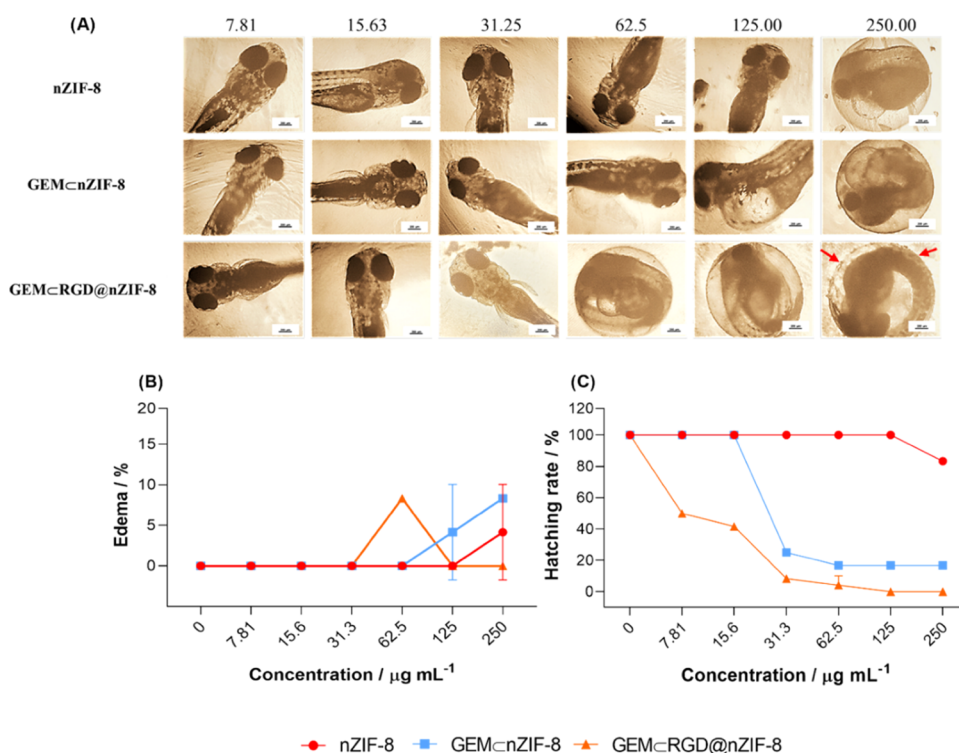
Figure 3. (A) Representative images of zebrafish embryo development showing (B) malformation and (C) different hatching rates after 96 h incubation with pure nZIF-8 (red), non-targeting GEM⊂nZIF-8 (blue), and cancer-targeting GEM⊂RGD@nZIF-8 (orange). Concentrations ranging from 0 to 250 μg mL^{-1} were applied with a total of 24 zebrafish embryos per concentration. Images were captured under an inverted microscope with a scale bar of 200 μm. Error bars represent standard deviation ($n = 2$).

targeting GEM⊂nZIF-8, and pure nZIF-8 demonstrate concentration-dependent toxicity toward zebrafish embryos after 96 h of incubation. Survivability of the embryos decreased significantly ($P < 0.001$) as the concentrations of the nanotherapeutics increased from 7.81 to 250 μg mL^{-1}. The highest concentration (250 μg mL^{-1}) of cancer-targeting GEM⊂RGD@nZIF-8 and non-targeting GEM⊂nZIF-8 exhibit a decreasing trend ($P < 0.001$) in survival rate at the 24–96 h mark (Figure 2E). Although both these nanotherapeutics illustrate a decrease in survivability, it was noted that cancer-targeting GEM⊂RGD@nZIF-8 had a significant survivability advantage ($P < 0.001$) with a 75% survival rate compared with non-targeting GEM⊂nZIF-8 (58.3% survival rate). This finding is exciting when correlated with the promising cell viability data reported in our previous work in which the percentage of viability in normal MRC-5 cells was significantly higher (63%; $P < 0.001$) than in cancerous A549 cells (25%) after 48 h of incubation with cancer-targeting GEM⊂RGD@nZIF-8.[16] It is noted that pure nZIF-8 showed the least toxicity as there was no significant difference ($P > 0.05$) in the survival rate when nZIF-8 was incubated with embryos for 24 until 96 h.[16] After this, the lethal concentration (LC$_{50}$) was quantified for each nanotherapeutic at its lethal endpoint of 96 h. LC$_{50}$ values were found to be more than 250 μg mL^{-1}, indicating that the concentrations tested are not toxic to healthy zebrafish embryos.

Next, malformations among surviving zebrafish embryos were evaluated after incubation with cancer-targeting GEM⊂RGD@nZIF-8, non-targeting GEM⊂nZIF-8, and pure nZIF-8 for 96 h using a concentration range of 7.81–250 μg mL^{-1} (Figure 3A,B). Overall, the surviving zebrafish embryos did not exhibit any sign of scoliosis. A low percentage of edema

(8.3%) was observed at only 62.5 μg mL^{-1} post-incubation with cancer-targeting GEM⊂RGD@nZIF-8. Meanwhile, for non-targeting GEM⊂nZIF-8, edema (4.2 and 8.3%) was observed at 125 and 250 μg mL^{-1}. At the higher concentrations (125 and 250 μg mL^{-1}), the nanocarrier aggregates around the porous chorion, which may decrease the nanocarrier permeation. The lack of toxicity demonstrated by our system is in contrast to previous reports that use either Cu-metal-organic framework (MOF) or MIL-101, in which those MOFs induced toxicity in zebrafish embryos owing to metal ion leaching during MOF degradation.[24,61]

Hatching rates were also studied to better understand the effects on zebrafish embryos upon incubation with cancer-targeting GEM⊂RGD@nZIF-8, non-targeting GEM⊂nZIF-8, and pure nZIF-8. As shown in Figure 3C, all zebrafish embryos hatched after incubation with pure nZIF-8 in concentrations ranging from 7.81 to 125 μg mL^{-1}. The hatching rate decreased only to 83.3% after applying the highest concentration (250 μg mL^{-1}) of pure nZIF-8. Contrastingly, cancer-targeting GEM⊂RGD@nZIF-8 and non-targeting GEM⊂nZIF-8 displayed concentration-dependent inhibition of zebrafish embryo hatching. Overall, the hatching rate of zebra embryos incubated with cancer-targeting GEM⊂RGD@nZIF-8 was lower than those incubated with non-targeting GEM⊂nZIF-8. The cancer-targeting GEM⊂RGD@nZIF-8 and non-targeting GEM⊂nZIF-8 start to inhibit zebrafish embryo hatching at concentrations as low as 7.81 μg mL^{-1} (50%) and 31.25 μg mL^{-1} (25%), respectively. The zebrafish embryos completely failed to hatch when incubated with higher concentrations (125 and 250 μg mL^{-1}) of cancer-targeting GEM⊂RGD@nZIF-8. The reason for this is that aggregates of the nanocarrier can form around the outermost

porous chorion, which leads to an alteration in its elasticity function (Figure 3A).[62] This is likely due to the fact that the key part of the hatching process is the secretion of a metalloprotease enzyme from the hatching gland.[63] Indeed, this process weakens the chorion and permits the embryo to escape. There have also been reports that functionalized nanocarriers can also interfere with the hatching process by inhibiting the enzyme[64] or by slowing the maturation of the hatching gland.[65] This mechanism can differ with a variety of chemical properties of functionalized agents and the employed concentration of the incubated nanocarriers.[66] Therefore, we emphasize that the data reported herein requires further study of the tested zebrafish embryo stage to obtain more information on its hatching profile.

It is important to note that, although GEM⊂RGD@nZIF-8 displayed an enhanced permeability, it is not necessary for a cancer-targeting nanotherapeutic to impair survivability in healthy zebrafish embryos. This can happen as a result of the RGD interaction with transient expression of $\alpha v\beta 3$ integrins within a certain period of time. In our study, the non-hatched embryos treated with GEM⊂RGD@nZIF-8 did not cause death, coagulation, lack of somite, and non-detachment of the tail, all of which are important parameters that determine survivability.[37]

CONCLUSIONS

In this report, we detailed the dissolution profile of nZIF-8, which provided an estimate of the pH responsiveness of this important nanotherapeutic system. With a similarity value (f_2) <50, the dissolution of cancer-targeting GEM⊂RGD@nZIF-8 was more pH-responsive and sustained in a tumor environment mimicking acidic media (PBS solution with pH = 6.0) than neutral media (PBS solution with pH = 7.4). A detailed dissolution kinetic study demonstrated that the Higuchi model played a role in determining the dissolution mechanism of GEM from the nanotherapeutic based on Fickian diffusion in both pH = 6.0 and 7.4 media. Furthermore, evidence was presented for an enhanced permeability rate within the chorion membrane of zebrafish embryo for cancer-targeting GEM⊂RGD@nZIF-8 as opposed to non-targeting GEM⊂nZIF-8. With respect to toxicity assessment, the cancer-targeting GEM⊂RGD@nZIF-8 demonstrated greater survivability of the zebrafish embryos due to its targeting effectiveness created upon RGD functionalization at the surface of GEM⊂nZIF-8. Minimal adverse side effects were evident with a low percentage of edema (8.3%) at only 62.5 μg mL^{-1}. Hatching failure was found at only higher concentrations of 125 and 250 μg mL^{-1}. When taken together, this study suggests that cancer-targeting GEM⊂RGD@nZIF-8 could serve as a viable cancer nanotherapeutic for cancer treatment due to its pH-responsive character, ability to protect the chemotherapeutic agent in physiologically relevant conditions, and non-toxicity to a healthy organism. GEM⊂RGD@nZIF-8 is a promising candidate to be further studied in rodents or relevant cancer models to determine its efficacy.

ASSOCIATED CONTENT

ⓈI Supporting Information

The Supporting Information is available free of charge at https://pubs.acs.org/doi/10.1021/acsbiomaterials.2c00186.

Characterization details, powder X-ray diffraction (PXRD), Fourier transform infrared spectroscopy (FT-IR), and transmission electron microscopy (TEM) for nZIF-8, GEM⊂nZIF-8, and GEM⊂RGD@nZIF-8. Zebrafish embryos analysis and kinetic model analysis of the dissolution profiles (PDF)

■ AUTHOR INFORMATION

Corresponding Author

Mohd Basyaruddin Abdul Rahman − *Integrated Chemical BioPhysics Research, Faculty of Science, Universiti Putra Malaysia (UPM), Serdang 43400 Selangor, Malaysia; UPM-MAKNA Cancer Laboratory, Institute of Bioscience, Universiti Putra Malaysia, Serdang 43400 Selangor, Malaysia; Foundry of Reticular Materials for Sustainability (FORMS), Institute of Advanced Technology, Universiti Putra Malaysia, Serdang 43400 Selangor, Malaysia;* ⓘ orcid.org/0000-0002-5665-2564; Email: basya@upm.edu.my

Authors

Nurul Akmarina Mohd Abdul Kamal − *Integrated Chemical BioPhysics Research, Faculty of Science, Universiti Putra Malaysia (UPM), Serdang 43400 Selangor, Malaysia; UPM-MAKNA Cancer Laboratory, Institute of Bioscience, Universiti Putra Malaysia, Serdang 43400 Selangor, Malaysia; Foundry of Reticular Materials for Sustainability (FORMS), Institute of Advanced Technology, Universiti Putra Malaysia, Serdang 43400 Selangor, Malaysia; Faculty of Chemical and Process Engineering Technology, Universiti Malaysia Pahang (UMP), Pekan 26600 Pahang, Malaysia*

Emilia Abdulmalek − *Integrated Chemical BioPhysics Research, Faculty of Science, Universiti Putra Malaysia (UPM), Serdang 43400 Selangor, Malaysia; Foundry of Reticular Materials for Sustainability (FORMS), Institute of Advanced Technology, Universiti Putra Malaysia, Serdang 43400 Selangor, Malaysia*

Sharida Fakurazi − *Department of Human Anatomy, Faculty of Medicine and Health Sciences, Universiti Putra Malaysia, Serdang 43400 Selangor, Malaysia*

Kyle E. Cordova − *Foundry of Reticular Materials for Sustainability (FORMS), Institute of Advanced Technology, Universiti Putra Malaysia, Serdang 43400 Selangor, Malaysia; Materials Discovery Research Unit, Advanced Research Centre, Royal Scientific Society, Amman 11941, Jordan;* ⓘ orcid.org/0000-0002-4988-0497

Complete contact information is available at:
https://pubs.acs.org/10.1021/acsbiomaterials.2c00186

Author Contributions

N.A.M.A.K. performed the formal analysis, methodology, investigation, data curation, and writing, reviewing, and editing of the original draft. E.A.M. performed the data curation, supervision, funding acquisition, and writing, reviewing, and editing of the original draft. S.F. performed the data curation, supervision, and writing, reviewing, and editing of the original draft. K.E.C. performed the formal analysis, data curation, and writing, review, and editing of the original draft. M.B.A.R. performed the conceptualization, supervision, funding acquisition, and writing, reviewing, and editing of the original draft. All authors have given approval to the final version of the manuscript.

Notes

The authors declare no competing financial interest.

■ REFERENCES

(1) Globocan. *The Global Cancer Observatory - All Cancers*, International Agency for Research on Cancer - WHO, 2020, pp 199-200.

(2) Feng, S. S.; Chien, S. Chemotherapeutic Engineering: Application and Further Development of Chemical Engineering Principles for Chemotherapy of Cancer and Other Diseases. *Chem. Eng. Sci.* 2003, 58, 4087−4114.

(3) Bai, J.; Peng, C.; Guo, L.; Zhou, M. Metal-Organic Framework-Integrated Enzymes as Bioreactor for Enhanced Therapy against Solid Tumor via a Cascade Catalytic Reaction. *ACS Biomater. Sci. Eng.* 2019, 5, 6207−6215.

(4) Gao, L.; Wu, Z.; Ibrahim, A. R.; Zhou, S. F.; Zhan, G. Fabrication of Folic Acid-Decorated Hollow ZIF-8/Au/CuS Nanocomposites for Enhanced and Selective Anticancer Therapy. *ACS Biomater. Sci. Eng.* 2020, 6, 6095−6107.

(5) Zheng, M.; Liu, S.; Guan, X.; Xie, Z. One-Step Synthesis of Nanoscale Zeolitic Imidazolate Frameworks with High Curcumin Loading for Treatment of Cervical Cancer. *ACS Appl. Mater. Interfaces* 2015, 7, 22181−22187.

(6) He, M.; Zhou, J.; Chen, J.; Zheng, F.; Wang, D.; Shi, R.; Guo, Z.; Wang, H.; Chen, Q. Fe3O4@carbon@zeolitic Imidazolate Framework-8 Nanoparticles as Multifunctional PH-Responsive Drug Delivery Vehicles for Tumor Therapy in Vivo. *J. Mater. Chem. B* 2015, 3, 9033−9042.

(7) Li, S.; Wang, K.; Shi, Y.; Cui, Y.; Chen, B.; He, B.; Dai, W.; Zhang, H.; Wang, X.; Zhong, C.; Wu, H.; Yang, Q.; Zhang, Q. Novel Biological Functions of ZIF-NP as a Delivery Vehicle: High Pulmonary Accumulation, Favorable Biocompatibility, and Improved Therapeutic Outcome. *Adv. Funct. Mater.* 2016, 26, 2715−2727.

(8) Wang, S.; McGuirk, C. M.; d'Aquino, A.; Mason, J. A.; Mirkin, C. A. Metal−Organic Framework Nanoparticles. *Adv. Mater.* 2018, 30, No. 1800202.

(9) Lin, Y.; Zhong, Y.; Chen, Y.; Li, L.; Chen, G.; Zhang, J.; Li, P.; Zhou, C.; Sun, Y.; Ma, Y.; Xie, Z.; Liao, Q. Ligand-Modified Erythrocyte Membrane-Cloaked Metal-Organic Framework Nanoparticles for Targeted Antitumor Therapy. *Mol. Pharmaceutics* 2020, 17, 3328−3341.

(10) Hao, J.; Milašin, I. S.; Eken, Z. B. E.; Mravak-stipetic, M.; Pavelić, K.; Ozer, F. Effects of Zeolite as a Drug Delivery System on Cancer Therapy: A Systematic Review. *Molecules* 2021, 26, No. 6196.

(11) Yu, H.; Qiu, X.; Neelakanda, P.; Deng, L.; Khashab, N. M.; Nunes, S. P.; Peinemann, K. V. Hollow ZIF-8 Nanoworms from Block Copolymer Templates. *Sci. Rep.* 2015, 5, No. 15275.

(12) Li, Y.; Zheng, Y.; Lai, X.; Chu, Y.; Chen, Y. Biocompatible Surface Modification of Nano-Scale Zeolitic Imidazolate Frameworks for Enhanced Drug Delivery. *RSC Adv.* 2018, 8, 23623−23628.

(13) Ettlinger, R.; Moreno, N.; Volkmer, D.; Kerl, K.; Bunzen, H. Zeolitic Imidazolate Framework-8 as PH-Sensitive Nanocarrier for "Arsenic Trioxide. *Chem. - Eur. J.* 2019, 25, 13189−13196.

(14) Pang, J.; Xing, H.; Sun, Y.; Feng, S.; Wang, S. Non-Small Cell Lung Cancer Combination Therapy: Hyaluronic Acid Modified, Epidermal Growth Factor Receptor Targeted, PH Sensitive Lipid-Polymer Hybrid Nanoparticles for the Delivery of Erlotinib plus Bevacizumab. *Biomed. Pharmacother.* 2020, 125, No. 109861.

(15) Chowdhuri, A. R.; Laha, D.; Pal, S.; Karmakar, P.; Sahu, S. K. One-Pot Synthesis of Folic Acid Encapsulated Upconversion Nanoscale Metal Organic Frameworks for Targeting, Imaging and PH Responsive Drug Release. *Dalton Trans.* 2016, 45, 18120−18132.

(16) Kamal, N. A. M. A.; Abdulmalek, E.; Fakurazi, S.; Cordova, K. E.; Rahman, M. B. A. Surface Peptide Functionalization of Zeolitic Imidazolate Framework-8 for Autonomous Homing and Enhanced Delivery of Chemotherapeutic Agent to Lung Tumor Cells. *Dalton Trans.* 2021, 50, 2375−2386.

(17) Wang, J.; Bai, R.; Yang, R.; Liu, J.; Tang, J.; Liu, Y.; Li, J.; Chai, Z.; Chen, C. Size- and Surface Chemistry-Dependent Pharmacokinetics and Tumor Accumulation of Engineered Gold Nanoparticles after Intravenous Administration. *Metallomics* 2015, 7, 516−524.

(18) Yang, L.; Ho, N. Y.; Alshut, R.; Legradi, J.; Weiss, C.; Reischl, M.; Mikut, R.; Liebel, U.; Müller, F.; Strähle, U. Zebrafish Embryos as Models for Embryotoxic and Teratogenic Effects of Chemicals. *Reprod. Toxicol.* 2009, 28, 245−253.

(19) Howe, K.; Clark, M. D.; Torroja, C. F.; Torrance, J.; Berthelot, C.; Muffato, M.; Collins, J. E.; Humphray, S.; McLaren, K.; Matthews, L.; McLaren, S.; Sealy, I.; Caccamo, M.; Churcher, C.; Scott, C.; Barrett, J. C.; Koch, R.; Rauch, G. J.; White, S.; Chow, W.; Kilian, B.; Quintais, L. T.; Guerra-Assunção, J. A.; Zhou, Y.; Gu, Y.; Yen, J.; Vogel, J. H.; Eyre, T.; Redmond, S.; Banerjee, R.; Chi, J.; Fu, B.; Langley, E.; Maguire, S. F.; Laird, G. K.; Lloyd, D.; Kenyon, E.; Donaldson, S.; Sehra, H.; Almeida-King, J.; Loveland, J.; Trevanion, S.; Jones, M.; Quail, M.; Willey, D.; Hunt, A.; Burton, J.; Sims, S.; McLay, K.; Plumb, B.; Davis, J.; Clee, C.; Oliver, K.; Clark, R.; Riddle, C.; Eliott, D.; Threadgold, G.; Harden, G.; Ware, D.; Mortimore, B.; Kerry, G.; Heath, P.; Phillimore, B.; Tracey, A.; Corby, N.; Dunn, M.; Johnson, C.; Wood, J.; Clark, S.; Pelan, S.; Griffiths, G.; Smith, M.; Glithero, R.; Howden, P.; Barker, N.; Stevens, C.; Harley, J.; Holt, K.; Panagiotidis, G.; Lovell, J.; Beasley, H.; Henderson, C.; Gordon, D.; Auger, K.; Wright, D.; Collins, J.; Raisen, C.; Dyer, L.; Leung, K.; Robertson, L.; Ambridge, K.; Leongamornlert, D.; McGuire, S.; Gilderthorp, R.; Griffiths, C.; Manthravadi, D.; Nichol, S.; Barker, G.; Whitehead, S.; Kay, M.; Brown, J.; Murnane, C.; Gray, E.; Humphries, M.; Sycamore, N.; Barker, D.; Saunders, D.; Wallis, J.; Babbage, A.; Hammond, S.; Mashreghi-Mohammadi, M.; Barr, L.; Martin, S.; Wray, P.; Ellington, A.; Matthews, N.; Ellwood, M.; Woodmansey, R.; Clark, G.; Cooper, J.; Tromans, A.; Grafham, D.; Skuce, C.; Pandian, R.; Andrews, R.; Harrison, E.; Kimberley, A.; Garnett, J.; Fosker, N.; Hall, R.; Garner, P.; Kelly, D.; Bird, C.; Palmer, S.; Gehring, I.; Berger, A.; Dooley, C. M.; Ersan-Ürün, Z.; Eser, C.; Geiger, H.; Geisler, M.; Karotki, L.; Kirn, A.; Konantz, J.; Konantz, M.; Oberländer, M.; Rudolph-Geiger, S.; Teucke, M.; Osoegawa, K.; Zhu, B.; Rapp, A.; Widaa, S.; Langford, C.; Yang, F.; Carter, N. P.; Harrow, J.; Ning, Z.; Herrero, J.; Searle, S. M. J.; Enright, A.; Geisler, R.; Plasterk, R. H. A.; Lee, C.; Westerfield, M.; de Jong, P. J.; Zon, L. I.; Postlethwait, J. H.; Nüsslein-Volhard, C.; Hubbard, T. J. P.; Crollius, H. R.; Rogers, J.; Stemple, D. L.; et al. The Zebrafish Reference Genome Sequence and Its Relationship to the Human Genome. *Nature* 2013, 496, 498−503.

(20) Hason, M.; Bartůněk, P. Zebrafish Models of Cancer-New Insights on Modeling Human Cancer in a Non-Mammalian Vertebrate. *Genes* 2019, 10, No. 935.

(21) Patton, E. E.; Zon, L. I.; Langenau, D. M. Zebrafish Disease Models in Drug Discovery: From Preclinical Modelling to Clinical Trials. *Nat. Rev. Drug Discovery* 2021, 20, 611−628.

(22) Berghmans, S.; Butler, P.; Goldsmith, P.; Waldron, G.; Gardner, I.; Golder, Z.; Richards, F. M.; Kimber, G.; Roach, A.; Alderton, W.; Fleming, A. Zebrafish Based Assays for the Assessment of Cardiac, Visual and Gut Function - Potential Safety Screens for Early Drug Discovery. *J. Pharmacol. Toxicol. Methods* 2008, 58, 59−68.

(23) Pensado-López, A.; Fernández-Rey, J.; Reimunde, P.; Crecente-Campo, J.; Sánchez, L.; Andón, F. T. Zebrafish Models for the Safety and Therapeutic Testing of Nanoparticles with a Focus on Macrophages. *Nanomaterials* 2021, 11, No. 1784.

(24) Abramenko, N.; Deyko, G.; Abkhalimov, E.; Isaeva, V.; Pelgunova, L.; Krysanov, E.; Kustov, L. Acute Toxicity of Cu-Mof Nanoparticles (Nanohkust-1) towards Embryos and Adult Zebrafish. *Int. J. Mol. Sci.* 2021, 22, No. 5568.

(25) Jurewicz, A.; Ilyas, S.; Uppal, J. K.; Ivandic, I.; Korsching, S.; Mathur, S. Evaluation of Magnetite Nanoparticle-Based Toxicity on

Embryo-Larvae Stages of Zebrafish (*Danio rerio*). *ACS Appl. Nano Mater.* **2020**, *3*, 1621−1629.

(26) Haque, E.; Ward, A. Zebrafish as a Model to Evaluate Nanoparticle Toxicity. *Nanomaterials* **2018**, *8*, No. 561.

(27) Pyati, U. J.; Look, A. T.; Hammerschmidt, M. Zebrafish as a Powerful Vertebrate Model System for in Vivo Studies of Cell Death. *Semin. Cancer Biol.* **2007**, *17*, 154−165.

(28) Lin, H. S.; Huang, Y. L.; Wang, Y. R.; Hsiao, E.; Hsu, T. A.; Shiao, H. Y.; Jiaang, W. T.; Sampurna, B. P.; Lin, K. H.; Wu, M. S.; Lai, G. M.; Yuh, C. H. Identification of Novel Anti-Liver Cancer Small Molecules with Better Therapeutic Index than Sorafenib via Zebrafish Drug Screening Platform. *Cancers* **2019**, *11*, No. 739.

(29) Younes, N.; Pintus, G.; Al-Asmakh, M.; Rasool, K.; Younes, S.; Calzolari, S.; Mahmoud, K. A.; Nasrallah, G. K. "safe" Chitosan/Zinc Oxide Nanocomposite Has Minimal Organ-Specific Toxicity in Early Stages of Zebrafish Development. *ACS Biomater. Sci. Eng.* **2020**, *6*, 38−47.

(30) Toschi, L.; Finocchiaro, G.; Bartolini, S.; Gioia, V.; Cappuzzo, F. Role of Gemcitabine in Cancer Therapy. *Future Oncol.* **2005**, *1*, 7−17.

(31) Dong, K.; Wang, Z.; Zhang, Y.; Ren, J.; Qu, X. Metal-Organic Framework-Based Nanoplatform for Intracellular Environment-Responsive Endo/Lysosomal Escape and Enhanced Cancer Therapy. *ACS Appl. Mater. Interfaces* **2018**, *10*, 31998−32005.

(32) Bi, J.; Lu, Y.; Dong, Y.; Gao, P. Synthesis of Folic Acid-Modified DOX @ ZIF-8 Nanoparticles for Targeted Therapy of Liver Cancer. *J. Nanomater.* **2018**, *2018*, 1−5.

(33) Gohel, M. C.; Sarvaiya, K. G.; Shah, A. R.; Brahmbhatt, B. K. Mathematical Approach for the Assessment of Similarity Factor Using a New Scheme for Calculating Weight. *Indian J. Pharm. Sci.* **2009**, *71*, 142−144.

(34) Forbes, B.; Richer, N. H.; Buttini, F. Dissolution: A Critical Performance Characteristic of Inhaled Products? *Pulm. Drug Delivery* **2015**, 223−240.

(35) Paarakh, M. P.; Jose, P. A. N. I.; Setty, C. M.; Christoper, G. V. P. Release Kinetics − Concepts and Applications. *Int. J. Pharm. Res. Technol.* **2019**, *8*, 12−20.

(36) Bhattacharyya, S. K.; Dule, M.; Paul, R.; Dash, J.; Anas, M.; Mandal, T. K.; Das, P.; Das, N. C.; Banerjee, S. Carbon Dot Cross-Linked Gelatin Nanocomposite Hydrogel for PH-Sensing and PH-Responsive Drug Delivery. *ACS Biomater. Sci. Eng.* **2020**, *6*, 5662−5674.

(37) OECD. Guidelines for the Testing Chemicals, Section 2: Effects on Biotic Systems, Test No. 236: Fish, Embryo Acute Toxicity (FET) Test. **2013**, No. July, 1−22.

(38) Shaikh, A.; Kohale, K.; Ibrahim, M.; Khan, M. Teratogenic Effects of Aqueous Extract of Ficus Glomerata Leaf during Embryonic Development in Zebrafish (*Danio rerio*). *J. Appl. Pharm. Sci.* **2019**, *9*, 107−111.

(39) Wang, Q.; Sun, Y.; Li, S.; Zhang, P.; Yao, Q. Synthesis and Modification of ZIF-8 and Its Application in Drug Delivery and Tumor Therapy. *RSC Adv.* **2020**, *10*, 37600−37620.

(40) Hyun, S. M.; Lee, J. H.; Jung, G. Y.; Kim, Y. K.; Kim, T. K.; Jeoung, S.; Kwak, S. K.; Moon, D.; Moon, H. R. Exploration of Gate-Opening and Breathing Phenomena in a Tailored Flexible Metal-Organic Framework. *Inorg. Chem.* **2016**, *55*, 1920−1925.

(41) Sun, C. Y.; Qin, C.; Wang, X. L.; Yang, G. S.; Shao, K. Z.; Lan, Y. Q.; Su, Z. M.; Huang, P.; Wang, C. G.; Wang, E. B. Zeolitic Imidazolate Framework-8 as Efficient PH-Sensitive Drug Delivery Vehicle. *Dalton Trans.* **2012**, *41*, 6906−6909.

(42) Xia, Y.; Hong, Y.; Geng, R.; Li, X.; Qu, A.; Zhou, Z.; Zhang, Z. Amine-Functionalized ZIF-8 as a Fluorescent Probe for Breath Volatile Organic Compound Biomarker Detection of Lung Cancer Patients. *ACS Omega* **2020**, *5*, 3478−3486.

(43) de Moura Ferraz, L. R.; Tabosa, A. É. G. A.; da Silva Nascimento, D. D. S.; Ferreira, A. S.; de Albuquerque Wanderley Sales, V.; Silva, J. Y. R.; Júnior, S. A.; Rolim, L. A.; de Souza Pereira, J. J.; Rolim-Neto, P. J. ZIF-8 as a Promising Drug Delivery System for Benznidazole: Development, Characterization, in Vitro Dialysis Release and Cytotoxicity. *Sci. Rep.* **2020**, *10*, No. 16815.

(44) Taheri, M.; Tsuzuki, T. Photo-Accelerated Hydrolysis of Metal Organic Framework ZIF-8. *ACS Mater. Lett.* **2021**, *3*, 255−260.

(45) Esfahanian, M.; Ghasemzadeh, M. A.; Razavian, S. M. H. Synthesis, Identification and Application of the Novel Metal-Organic Framework Fe3O4@PAA@ZIF-8 for the Drug Delivery of Ciprofloxacin and Investigation of Antibacterial Activity. *Artif. Cells, Nanomed., Biotechnol.* **2019**, *47*, 2024−2030.

(46) Akbari, M.; Ghasemzadeh, M. A.; Fadaeian, M. Synthesis and Application of ZIF-8 MOF Incorporated in a TiO2@Chitosan Nanocomposite as a Strong Nanocarrier for the Drug Delivery of Acyclovir. *ChemistrySelect* **2020**, *5*, 14564−14571.

(47) Huang, Z.-g.; Lv, F.-m.; Wang, J.; Cao, S.-j.; Liu, Z.-p.; Liu, Y.; Lu, W.-y. RGD-Modified PEGylated Paclitaxel Nanocrystals with Enhanced Stability and Tumor-Targeting Capability. *Int. J. Pharm.* **2019**, *556*, 217−225.

(48) Jin, X.; Zhou, J.; Zhang, Z.; Lv, H. Doxorubicin Combined with Betulinic Acid or Lonidamine in RGD Ligand- Targeted PH-Sensitive Micellar System for Ovarian Cancer Treatment Department of Pharmaceutics, State Key Laboratory of Natural Medicines, China Jiangsu Province Hospital on Integrati. *Int. J. Pharm.* **2019**, No. 118751.

(49) Fenaroli, F.; Westmoreland, D.; Benjaminsen, J.; Kolstad, T.; Skjeldal, F. M.; Meijer, A. H.; van der Vaart, M.; Ulanova, L.; Roos, N.; Nyström, B.; Hildahl, J.; Griffiths, G. Nanoparticles as Drug Delivery System against Tuberculosis in Zebrafish Embryos: Direct Visualization and Treatment. *ACS Nano* **2014**, *8*, 7014−7026.

(50) Hagedorn, M.; Kleinhans, F. W.; Artemov, D.; Pilatus, U. Characterization of a Major Permeability Barrier in the Zebrafish Embryo. *Biol. Reprod.* **1998**, *59*, 1240−1250.

(51) Villalobos, S. A.; Hamm, J. T.; Teh, S. J.; Hinton, D. E. Thiobencarb-Induced Embryotoxicity in Medaka (Oryzias Latipes): Stage- Specific Toxicity and the Protective Role of Chorion. *Aquat. Toxicol.* **2000**, *48*, 309−326.

(52) Gellert, G.; Heinrichsdorff, J. Effect of Age on the Susceptibility of Zebrafish Eggs to Industrial Wastewater. *Water Res.* **2001**, *35*, 3754−3757.

(53) Gibson, J. A Functional Characterisation of the Dimerisation Motif in Fibronectin, in Vivo and in Vitro. Ph.D Dissertation, Ludwig Maximilian University of Munich, München, Germany, 2014.

(54) Ablooglu, A. J.; Kang, J.; Handin, R. I.; Traver, D.; Shattil, S. J. The Zebrafish Vitronectin Receptor: Characterization of Integrin AV and B3 Expression Patterns in Early Vertebrate Development. *Dev. Dyn.* **2007**, *236*, 2268−2276.

(55) Wang, J.; Li, W.; Lu, Z.; Zhang, L.; Hu, Y.; Li, Q.; Du, W.; Feng, X.; Jia, H.; Liu, B. F. The Use of RGD-Engineered Exosomes for Enhanced Targeting Ability and Synergistic Therapy toward Angiogenesis. *Nanoscale* **2017**, *9*, 15598−15605.

(56) Calderwood, D. A. Integrin Activation. *J. Cell Sci.* **2004**, *117*, 657−666.

(57) van Agthoven, J. F.; Xiong, J. P.; Alonso, J. L.; Rui, X.; Adair, B. D.; Goodman, S. L.; Arnaout, M. A. Structural Basis for Pure Antagonism of Integrin α Vβ 3 by a High-Affinity Form of Fibronectin. *Nat. Struct. Mol. Biol.* **2014**, *21*, 383−388.

(58) Luo, B. H.; Carman, C. V.; Springer, T. A. Structural Basis of Integrin Regulation and Signaling. *Annu. Rev. Immunol.* **2007**, *25*, 619−647.

(59) Mohammed, A.; Halfhide, T.; Elias-Samlalsingh, N. Comparative Sensitivity of Three Life Stages of the Tropical Mysid, Metamysidopsis Insularis to Six Toxicants. *Toxicol. Environ. Chem.* **2009**, *91*, 1331−1337.

(60) Vasconcelos, V.; Azevedo, J.; Silva, M.; Ramos, V. Effects of Marine Toxins on the Reproduction and Early Stages Development of Aquatic Organisms. *Mar. Drugs* **2010**, *8*, 59−79.

(61) Ruyra, À.; Yazdi, A.; Espín, J.; Carné-Sánchez, A.; Roher, N.; Lorenzo, J.; Imaz, I.; Maspoch, D. Synthesis, Culture Medium Stability, and in Vitro and in Vivo Zebrafish Embryo Toxicity of

Metal-Organic Framework Nanoparticles. *Chem. - Eur. J.* **2015**, *21*, 2508−2518.
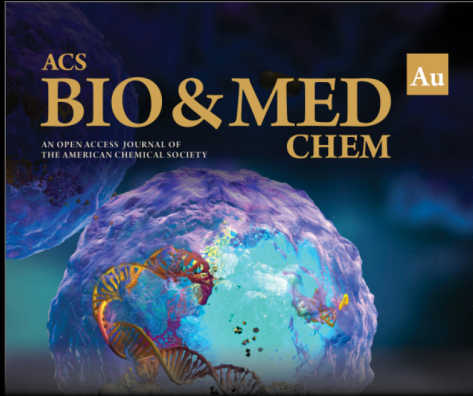
(62) Cheng, J.; Flahaut, E.; Shuk, H. C. Effect of Carbon Nanotubes on Developing Zebrafish (*Danio rerio*) Embryos. *Environ. Toxicol. Chem.* **2007**, *26*, 708−716.

(63) Sano, K.; Inohaya, K.; Kawaguchi, M.; Yoshizaki, N.; Iuchi, I.; Yasumasu, S. Purification and Characterization of Zebrafish Hatching Enzyme - An Evolutionary Aspect of the Mechanism of Egg Envelope Digestion. *FEBS J.* **2008**, *275*, 5934−5946.

(64) MacCormack, T. J.; Clark, R. J.; Dang, M. K. M.; Ma, G.; Kelly, J. A.; Veinot, J. G. C.; Goss, G. G. Inhibition of Enzyme Activity by Nanomaterials: Potential Mechanisms and Implications for Nano-toxicity Testing. *Nanotoxicology* **2012**, *6*, 514−525.

(65) Yamagami, K. Mechanisms of Hatching in Fish: Secretion of Hatching Enzyme and Enzymatic Choriolysis. *Am. Zool.* **1981**, *21*, 459−471.

(66) Hansjosten, I.; Takamiya, M.; Rapp, J.; Reiner, L.; Fritsch-Decker, S.; Mattern, D.; Andraschko, S.; Anders, C.; Pace, G.; Dickmeis, T.; Peravali, R.; Rastegar, S.; Strähle, U.; Hsiao, I.-L.; Gilliland, D.; Ojea-Jimenez, I.; Ambrose, S. V. Y.; Belinga-Desaunay-Nault, M.-F. A.; Khan, A. O.; Lynch, I.; Valsami-Jones, E.; Diabaté, S.; Weiss, C. Surface Functionalisation-Dependent Adverse Effects of Metal Nanoparticles and Nanoplastics in Zebrafish Embryos. *Environ. Sci. Nano* **2022**, *9*, 375−392.